第 27卷第 1期
2008年 2月

红 外 与 毫 米 波 学 报
J. Infrared Millim. Waves

Vol. 27, No. 1
February, 2008

文章编号: 1001 - 9014(2008)01 - 0001 - 06

RECENT PROGRESS AND POTENTIAL IMPACT OF MODULATION SPECTROSCOPY FOR NARROW-GAP HgCdTe

SHAO Jun[1], MA Li-Li[1], LÜ Xiang[1], WU Jun[2], LI Zhi-Feng[1],
GUO Shao-Ling[1], HE Li[2], LU Wei[1], CHU Jun-Hao[1,3]

(1. National Laboratory for Infrared Physics, Shanghai Institute of Technical Physics, Chinese Academy of Sciences, Shanghai 200083, China;
2. Research Center for Advanced Materials and Devices, Shanghai Institute of Technical Physics, Chinese Academy of Sciences, Shanghai 200083, China;
3. ECNU-SITP Joint Laboratory for Image Information, East China Normal University, Shanghai 200062, China)

Abstract: Recent progress of infrared photoreflectance and modulated photoluminescence techniques was outlined with special attention focused on the significant improvement of signal-to-noise ratio, spectral resolution and time consumption relative to the conventional techniques. Application of these techniques to molecular beam epitaxially grown HgCdTe films was given as examples, from which the potential impact of the techniques was foreseen on the optical study of narrow-gap semiconductors and inter-subband transition of wide-gap semiconductors with low-dimensional structures.

Key words: step-scan FTIR spectrometer; infrared photoreflectance; modulated photoluminescence; signal-to-noise ratio; spectral resolution

CLC number: O433.1, O657.33 **Document:** A

窄禁带碲镉汞调制光谱的近期进展和前景

邵 军[1], 马丽丽[1], 吕 翔[1], 吴 俊[2], 李志峰[1],
郭少令[1], 何 力[2], 陆 卫[1], 褚君浩[1,3]

(1. 中科院上海技术物理研究所红外物理国家实验室, 上海 200083;
2. 中科院上海技术物理所材器中心, 上海 200083;
3. 华东师范大学成像信息联合实验室, 上海 200062)

摘要: 简要介绍了红外光调制反射谱和调制光致发光谱的最新进展, 并重点比较了相对于传统实验方法在信噪比, 谱分辨率和实验耗时等方面所取得的显著进展. 给出了在 MBE生长 HgCdTe薄膜样品研究中的应用实例, 显示了该技术在光谱研究窄禁带半导体带间和低维结构带内跃迁方面的应用前景.

关 键 词: 步进扫描傅立叶变换红外光谱仪; 红外光调制反射; 调制光致发光; 信噪比, 谱分辨率

Introduction

$Hg_{1-x}Cd_xTe$ as a narrow-gap semiconductor has found wide applications in infrared (IR) detection. The device performances depend on the composition and the possible defects/impurities of the materials the device is made from. For identifying the energetic positions of the defects/impurities, electrical techniques

Received date: 2007-10-22, **revised date:** 2007-12-25 **收稿日期**: 2007-10-22, **修回日期**: 2007-12-25

Foudantion item: Supported by the national Natural Science Foundation of China (60676063), the Science and Technology Commssion of Shanghai Municipality (05ZR14133, 06JC14072), and the Knowledge Innovation Program of Chinese Academy of Sciences

Biography: SHAO Jun (1965-), male, Jiang-Su, China, Professor. Research area is optical spectroscopy and semiconductor physics.

were widely employed[1~6], though they could only provide information on charged impurities. Photoluminescence (PL)[7] and photoreflectance (PR) are both powerful nondestructive optical spectroscopic techniques. They have been employed widely in studies of optical properties of wide-gap semiconductors and drastically advanced the understanding of the optoelectronic characteristics of related materials[8~13]. However, both the conventional PL and PR experience tough limitation when application to mid- and far-IR spectral regions is desirable[14~16]. A direct consequence is that PL and PR were hardly used in the study of narrow-gap HgCdTe.

In near-IR spectral region, PL spectroscopy is usually based on a continuous-scan Fourier Transform Infrared (FTIR) spectrometer[17], due mainly to the well-known *multiplexing advantage* of using a single detector to measure all of the signals simultaneously and *throughput advantage* of sharing noise from this detector among all of the recorded signals equally[18,19]. In mid- and far-IR spectral regions, double-modulation PL techniques were developed for the sake of eliminating environmental thermal background emission centered around 10μm at room temperature[20~22]. As a trade-off, however, the PL measurement was very time consuming, and both the signal-to-noise ratio (SNR) and spectral resolution were poor.

The situation for PR spectroscopy is rather different. A conventional PR is usually based on a dispersive monochromator. The basic principle behind is to take derivative of optical spectrum with respect to the pump-beam induced modulation of built-in electric field near the sample surface. The derivative nature of PR spectrum suppresses unwanted background effects and emphasizes structures located in the energy range of inter-band transitions and other weak features that may not be seen in a normal optical reflectivity spectrum[23]. Such a powerful technique was, however, not applicable till very recent days to the spectral regions with wavelength longer than 4 μm[24,25], due to intrinsic limitations[15,26]. An attempt was reported of pushing PR measurement out to longer wavelengths by a technique based on a continuous-scan FTIR spectrometer[15]. However, the spectrum contained not only the material-related ΔR information but also the system response contributed by source, detector, etc., and even worse were the miserable SNR and spectral resolution, which indeed could not warrant a quantitative analysis[15].

In this regard, new conceptional modulated PL and IR PR techniques have been recently developed based on a step-scan FTIR spectrometer[14,16,26], which manifest in IR spectral regions significantly enhanced SNR and spectral resolution, and obviously shortened time consumption[14,26]. Especially, this PR technique breaks successfully the long-wavelength limitation of 4μm, and is applicable for quantitative analysis in the mid- and far-IR spectral regions[16].

1 Modulated PL by step-scan FTIR spectrometer

For the previous continuous-scan FTIR-based double-modulation PL technique proposed by Reisinger *et al*[20], the workflow of PL spectrum acquisition was similar to the conventional FTIR PL in the sense of continuous scan of the scanner, but with two major exceptions that (i) the pumping light was modulated by a chopper, of which the rotation frequency is referenced to a lock-in amplifier (LIA), and (ii) the output of the FTIR's detector was first fed to the LIA for demodulation and the output of the LIA was then fed into the FTIR for further treatment.

The word "double-modulation" came in due to the fact that besides the external modulation by chopper, the scanner of the FTIR did perform an internal "intrinsic" modulation when it moved continuously, its frequency depended on both the velocity of the scanner V (in cm/s) and the light energy ν (in cm^{-1}), which was known as "Fourier frequency" f_{FTIR}, $f_{FTIR} = 2V\nu$.

In fact, tough limitations in promoting SNR and spectral resolution are resulted in just because of the "double-modulation". On one hand, neither the available chopper nor the FTIR's detector allows too high external frequency. For a common mechanical chopper, the highest f_{chop} is about 4 KHz. The Fourier frequency and hence the scanner velocity must be low enough as a condition of $f_{chop}/f_{FTIR} \geq 10$ is required for a good separation of the two frequencies. The advantage

of quick measurement is thus lost. On the other hand, the time constant of the LIA must be significantly large relative to the chopper frequency while obviously small relative to the highest Fourier frequency, which can in practice be selected only in a very narrow time window of $10^{-1} \sim 10^{0}$ ms. This restrains the applicability severely because in most cases IR PL is so weak that the LIA needs a time constant of at least longer than 10 ms for working correctly.

For the modulated step-scan FTIR PL technique in our lab[14], an important difference is that the scanner of the FTIR spectrometer moves stepwise and the data acquisition takes place when the scanner stays at rest[27,28]. The advantages are that the external modulation frequency does not need to be so high and hence a common mechanical chopper works, and the problem of separating two modulation frequencies does not exist anymore, and the time constant can be selected as long as necessary. It ensures a successful resolution of the compromise among modulation frequency, scanner velocity, and LIA time constant.

Figure 1 depicts representative PL spectra recorded by either conventional FTIR PL [(a)] or modulated step-scan FTIR PL [(b) and (c)] technique for narrow-gap $Hg_{1-x}Cd_xTe$ films prepared by molecular beam epitaxy (MBE). The sample's temperature is kept at 77 K by a liquid-nitrogen dewar. The spectral resolution is 12 cm^{-1}. The time constant is set so that the modulated PL spectrum illustrated can be obtained within 3～10 minutes.

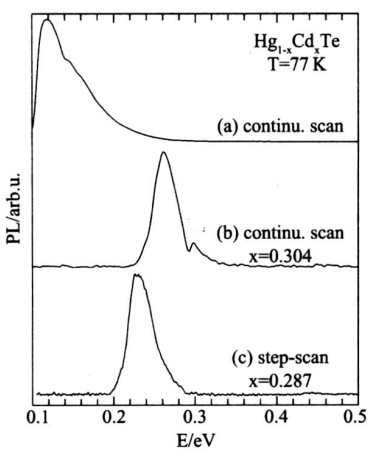

Fig 1 PL spectra by conventional FTIR PL method (a), and modulated step-scan FTIR PL technique for $Hg_{1-x}Cd_xTe$ thin film with (b) $x = 0.304$ and (c) $x = 0.287$. The PL peaks at around 0.26 eV for (b) and 0.23 eV for (c) are ascribed to HgCdTe-related transitions

图 1 $Hg_{1-x}Cd_xTe$样品的光致发光谱 (a)传统方法的测量结果 (b) (c) 基于 FTIR步进模式得到的光谱. 其中 (b) $x = 0.304$, (c) $x = 0.287$. (b) 图中 0.26 eV和 (c)中 0.23 eV处分别对应 HgCdTe相关跃迁

The spectrum in Fig. 1(a) manifests a strong peak around 0.12 eV due to the background thermal emission. Meanwhile, no evidence can be traced out at about 0.26 eV where PL signal from the $Hg_{1-x}Cd_xTe$ sample with $x = 0.304$ should locate[29]. The spectrum in Fig. 1(b), on the other hand, is flat around 0.12 eV, but does show a strong feature around 0.26 eV. In Fig. 1(c), PL spectrum from another $Hg_{1-x}Cd_xTe$ sample with slightly lower Cd content of $x = 0.287$ is depicted. A distinct PL feature can be seen around 0.23 eV, which is very close to the band gap for this Cd composition[29]. Therefore, the PL spectra in (b) and (c) reveal the band edge related PL transition with a SNR better than 40:1 while remove the disturbance of the thermal background emission totally.

For a comprehensive comparison, the work by Reisinger *et al.* is taken as a good example for the double-modulation PL methods[20]. In Fig. 6 of Ref. 20, the PL spectrum was obtained by 500 scans with the scanner velocity of 0.0355 cm/s and a spectral resolution of 10 cm^{-1}. The time consumption was hence estimated to be at least 25 minutes. The SNR of the PL spectrum was, however, estimated to be less than 5:1.

Taking the fact into account that SNR is approximately proportional to the square root of time consumption, we may make judgments that the modulated step-scan FTIR PL technique can (i) warrant a similar result as the previous double-modulation continuous-scan FTIR PL did within 1 minute, which is only 1/25 of the previous technique's time consumption, or (ii) achieve a SNR at least 15 times better than the previous double-modulation continuous-scan FTIR PL did within a similar experimental time consumption. These significant enhancements will warrant a reliable and systematic PL study of both temperature and excitation power effects on the PL property of HgCdTe materials.

2 IR PR by step-scan FTIR spectrometer

A conventional PR system consists of a mono-

chromator as a key part, together with pump light (usually a laser) and probe light (usually a wide-band) source, and a set of chopper and LIA. The intrinsic features of monochromator, IR detector and probe light source foreordain that this technique could not be extended to the IR spectral region with wavelength longer than 4 μm[24,25].

As the only attempt in extending PR technique to longer wavelength before the step-scan FTIR-based one emerges, a continuous-scan FTIR spectrometer was employed, and the intrinsic restriction again applied[15]. The spectrum was not normalized and therefore contained system response and possibly environmental disturbance, the SNR and spectral resolution were miserable and unreliable for quantitative analysis. These issues jointing together cast strong limitation on the real usefulness of the technique[15].

The step-scan FTIR spectrometer-based PR technique in our lab[16,26] breaks down the long-wavelength limitation successfully. Significant advances occur in two distinct aspects. Firstly, it brings the advantages of FTIR technique into full play, and thus enhances relative to the conventional PR technique the detectivity on one hand and removes the possible disturbance of either diffused reflected pump light and PL from the pumped sample or environmental instability on the other hand[8,30,31]. Secondly, it in principle does not need special consideration with respect to the FTIR spectrometer, and relaxes the limitation on the select of modulation frequency for the pump light and time constant for the LIA, relative to the continuous-scan FTIR PR attempt[15]. This ensures a drastic improvement of the SNR, spectral resolution as well as the time consumption.

Figure 2 illustrates PR measurement for an MBE-grown $Hg_{1-x}Cd_xTe$ sample with the step-scan FTIR PR technique. The R (a) and △R (b) are depicted at the same time with the final PR (c) spectrum. It is obvious that both the R and △R suffer from the disturbance of H_2O and CO_2 absorption as indicated by vertical dashes and arrows. This type of disturbance is, however, eliminated in the final PR spectrum because both R and △R are recorded respectively simultaneously. The main features at about 0.3 eV are probably

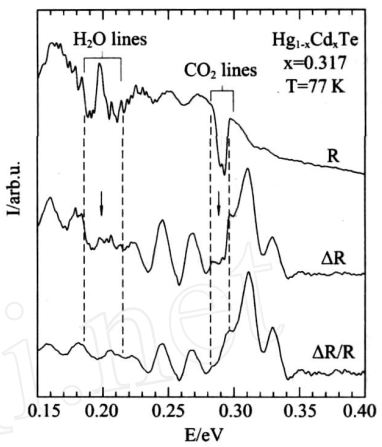

Fig 2 PR measurement for a MBE-grown $Hg_{1-x}Cd_xTe$ sample with step-scan FTIR PR technique: (a) static reflectivity R (b) the change △R, and (c) the final PR spectrum △R/R

图 2 基于 FTIR步进扫描模式的 PR方法得到的 MBE 生长 $Hg_{1-x}Cd_xTe$样品的光调制反射谱. (a) 静态反射信号 R, (b) 调制反射变化信号 △R, (c) 通过 △R/R 计算最终得到的 PR光谱

due to the band-to-band transition of the $Hg_{1-x}Cd_xTe$ sample, according to temperature-dependent empirical relation for band-gap energy [29].

It is noteworthy that the PR spectra illustrated in Fig 2 and 3 were recorded by a resolution of 8 cm^{-1} within 15 minutes. The SNR's are in the range of (13～40):1. The spectra, e.g., illustrated in Fig 6 of Ref. 15 and Fig 2 of Ref. 32, were recorded/depicted only in a very limited spectral range, from which SNR could not be reliably determined, and no hint was presented about the time consumption. Nevertheless, the separation between two adjacent data points is identifiable from the spectra, and the spectral resolution can hence be estimated to be at least worse than 200 cm^{-1}. This value was over 25 times as large as that is used in the step-scan FTIR PR measurements in the similar spectral region. It may hint extremely high time consumption for improving the spectral resolution if the improvement was not impossible, and indicate unambiguously that the spectrum recorded by the continuous-scan FTIR PR attempt can not be used for quantitative analyses even if a phenomenological discussion could be conducted. These facts warrant the step-scan FTIR PR a reliable, feasible and the only functional technique in the mid-and far-IR spectral regions.

3 Application on narrow-gap HgCdTe

A straightforward but important application of IR PR and modulated PL on narrow-gap HgCdTe is for the band-edge electronic structures, e. g , band gap and impurity/defect levels. Especially, the combination of the two techniques may ensure a characterization of both donor-and acceptor-like impurities reliably, and hence provide a pathway for the study of amphoteric behavior of arsenic doping in HgCdTe.

Figure 3 shows a modulated PL spectrum together with its curve fittings for a MBE-grown $Hg_{1-x}Cd_xTe$ sample at a temperature of 11K. The line shape of the PL spectrum is asymmetric with obvious shoulders on both sides. The SNR and spectral resolution are so good that theoretical treatment, e. g , curve fitting, can be performed reliably. The result indicates that such a line shape can be well fitted with three Gaussian lines as plotted in dashes in Fig. 3, the energy and intensity of each reveal the properties of related transition. From this procedure and combining with, e. g , temperature- and/or excitation power-dependent measurements, the band-to-band and shallow-level related transitions can be investigated and the information on the band gap and impurity levels may be extracted.

In Fig. 4(a), a PR spectrum is illustrated in dots for the same $Hg_{1-x}Cd_xTe$ sample at 150 K. To draw information about near band-edge electronic structures, least-square curve fittings are performed based on a third-derivative line-shape function for unbound situation and low electrical field modulation[9, 16]

$$\frac{\Delta R}{R} = \mathrm{Re}\sum_{i=1}^{n} A_i e^{j\phi_i}(E - E_i + j\Gamma_i)^{-2.5} \quad ,$$

where A_i and ϕ_i are the amplitude and phase of the line shape, E_i and Γ_i are the energy and broadening parameter of the particular transition, respectively. The fitting result is plotted in solid line and the critical energies are marked by vertical arrows in Fig. 4(a). Clearly, the PR spectrum manifests more information than the PL spectrum, especially in the energy range below the band gap. These critical points are related to both shallow- and deep-level impurities, according to their energies and separations[33].

Experimental support to this judgment is illustrated in Fig. 4(b), in which the PR spectra are recorded at a temperature of 77 K for three HgCdTe samples with different doping and annealing treatments. It is clearly seen that the main peak energy and the PR line shape as well are different from sample to sample, especially, the difference in low energy side is drastic [29]. This indicates that PR can distinguish quite well slight difference resulted in by sample's preparation and/or post-growth treatment.

As PR measurement can be performed effectively at both high and low temperatures, systematic analysis

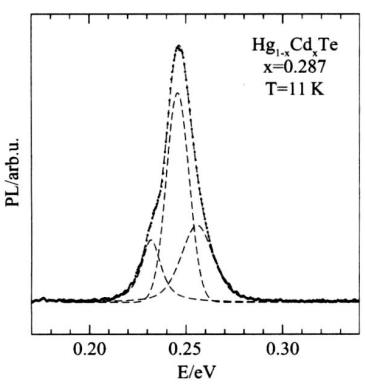

Fig. 3 PL spectrum and its curve fitting for a MBE-grown $Hg_{1-x}Cd_xTe$ sample at 11 K. Dashes represent the components of an optimized fitting

图 3 MBE生长 $Hg_{1-x}Cd_xTe$样品在 11K时的光致发光谱. 虚线是实验数据的拟合结果

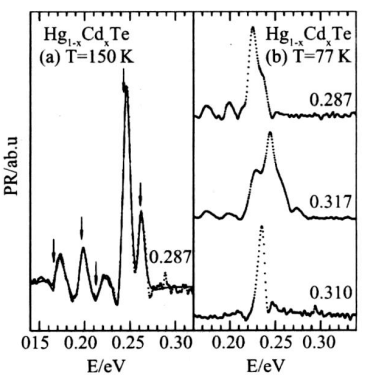

Fig. 4 PR spectrum for MBE-grown $Hg_{1-x}Cd_xTe$ sample (a) at 150 K for x = 0.287 in dots, and (b) at 77 K for x = 0.287, 0.317, and 0.310, respectively. Line-shape fitting is plotted in solid line in (a), the critical energies are marked by vertical arrows, and the highest energy corresponds to band gap

图 4 MBE生长 $Hg_{1-x}Cd_xTe$样品 PR谱. (a) x = 0.287样品在 150K时的 PR谱. (b) x = 0.287, 0.317和 0.310样品在 77K时的 PR谱. (a) 中实线是线形拟合的结果,拟合的能级位置已用箭头在对应位置标出,最高能量位置对应样品的禁带宽度

of temperature-dependent PR spectra will reveal not only a complete map of band-edge electronic structure but also its evolution with temperature. It is therefore expected to play a significant role in renewing the activity in optical study of narrow-gap HgCdTe. Furthermore, the IR PR may also find right application in the study of inter-subband transitions in wide-band semiconductors with low-dimensional structures, in the view of recent IR PR measurements on InAs/GaAs quantum-dot materials designed for quantum dot IR detector application.

Summary

To summarize, recent progress in IR PR and modulated PL techniques are outlined, with main interest focused on the improvement to the parameters of spectral SNR, resolution and time consumption relative to previous continuous-scan FTIR-based PR and double-modulation PL techniques, respectively. The results indicate that the new techniques can warrant at least one order of magnitude improvement to the parameters. Preliminary applications on MBE-grown HgCdTe films show that these techniques may ensure detailed study of band-edge electronic structures and doping/annealing dependence. Such progress is expected to play a key role in renewing activities in optical study of narrow-gap HgCdTe.

One of the authors (JS) thanks Guoliang Shi for technical supports. The assistance from F. Y. Yue and W. Huang in the early stage is acknowledged.

REFERENCES

[1] Zandian M, Chen A C, Edwall D D, *et al* *p*-type arsenic doping of $Hg_{1-x}Cd_xTe$ by molecular beam epitaxy[J]. *Appl Phys Lett* 1997, **71**, 2815.

[2] Shi X H, Rujirawat S, Ashokan R, *et al* Ionization energy of acceptors in As-doped HgCdTe grown by molecular beam epitaxy[J]. *Appl Phys Lett* 1998, **73**, 638.

[3] Selamet Y, Grein C H, Lee T S, *et al* Electrical properties of in situ As doped $Hg_{1-x}Cd_xTe$ epilayers grown by molecular beam epitaxy[J]. *J. Vac Sci Technol B*, 2001, **19**, 1488.

[4] Swartz C H, Tompkins R P, Giles N C, *et al* Infrared photoreflectance of InAs[J]. *J. Electronic Mat* 2004, **33**, 728.

[5] QUAN Zhi-Jue, LI Zhi-Feng, HU Wei-Da, *et al* Parameters extraction from the dark current characteristics of long-wavelength HgCdTe photodiode[J]. *J. Infrared Millim. Waves*(全知觉,李志锋,胡伟达,等. 光伏型碲镉汞长波探测器暗电流特性的参数提取研究. 红外毫米波学报), 2007, **26** (2): 92.

[6] XU Xiang-Yan, YE Zheng-Hua, LI Zhi-Feng, *et al* Numerical modeling of middle wavelength two color photovoltaic HgCdTe Detectors[J]. *J. Infrared Millim. Waves*(徐向晏,叶振华,李志锋,等. 中波双色光伏型 HgCdTe红外探测器模拟研究. 红外毫米波学报), 2007, **26** (3): 164.

[7] Hunter A T, McGill T C. Luminescence studies of HgCdTe alloys[J]. *J. Vac Sci Technol* 1982, **21**, 205.

[8] Shen H, Parayanthal P, Liu Y F, *et al* Pollak, New normalization procedure for modulation spectroscopy[J]. *Rev. Sci Instrum.* 1987, **58**, 1429.

[9] Pollak F H, Shen H. Modulation spectroscopy of semiconductors: bulk/thin film, microstructures, surfaces/interfaces and devices[J]. *Mater. Sci Eng.* 1993, **10**, 275.

[10] Klar P J, Rowland G, Thomas P J S, *et al* Photomodulated reflectance study of $In_xGa_{1-x}As/GaAs/AlAs$ microcavity vertical-cavity surface emitting laser structures in the weak-coupling regime: The cavity/ground-state-exciton resonance[J]. *Phys Rev. B*, 1999, **59**, 2894.

[11] Shao J, DÖemen A, Baars E, *et al* Photoluminescence and absorption identification of Ti^{3+} in zinc telluride[J], *Semicond. Sci Technol* 2002, **17**, 1213.

[12] Misiewicz J, Kudrawiec R, Ryczko K, *et al*, Photoreflectance investigations of the energy level structure in GaInNAs-based quantum wells[J]. *J. Phys : Condens Matter*, 2004, **16**, S3071.

[13] Shao J, LüX, Yue F, *et al*, Magnetophotoluminescence study of $Ga_xIn_{1-x}P$ quantum wells with CuPt-type long-range ordering[J]. *J. Appl Phys* 2006, **100**, 053522.

[14] Shao J, LuW, LüX, *et al* Modulated photoluminescence spectroscopy with a step-scan Fourier transform infrared spectrometer[J]. *Rev. Sci Instrum.* 2006, **77**, 063104.

[15] Hosea T J C, Merrick M, Murdin B N. A new Fourier transform photo-modulation spectroscopic technique for narrow band-gap materials in the mid- to far-infra-red[J]. *Phys Stat Sol* (a), 2005, **202**, 1233.

[16] Shao J, Yue F, LüX, *et al* Photomodulated infrared spectroscopy by a step-scan Fourier transform infrared spectrometer[J]. *Appl Phys Lett* 2006, **89**, 182121.

[17] Bignazzi A, Grilli E, Radice M, *et al* Fourier transform spectroscopy applied to photoluminescence: Advantages and warnings[J], *Rev. Sci Instrum.* 1996, **67**, 666.

[18] Smith B C. *Fundamentals of Fourier Transform Infrared Spectroscopy*[M]. Florida: CRC Press, Inc: 1996.

[19] Williams R. *Spectroscopy and the Fourier Transform: An interactive tutorial*[M]. New York: VCH, 1996.

[20] Reisinger A R, Roberts R N, Chinn S R, *et al* Photoluminescence of infrared-sensing materials using an FTIR spectrometer[J]. *Rev. Sci Instrum.* 1989, **60**, 82.

[21] Fuchs F, Lusson A, Wagner J, *et al* Double modulation techniques in fourier transform infrared photoluminescence [J]. *Proc SPIE*, 1989, **1145**, 323.

[22] Chang Y, Chu J H, Tang W G, *et al* Photoluminescence investigation on impurity behavior in Sb-doped HgCdTe [J], *Infrared Phys Technol*, 1996, **37**, 747.

[23] Shao J, Doemen A, Winterhoff R, *et al* Ordering parameter and band-offset determination for ordered $Ga_xIn_{1-x}P/(Al_{0.66}Ga_{0.34})_yIn_{1-y}P$ quantum wells[J]. *Phys Rev. B*, 2002, **66**, 035109.

(下转 20页)

耗波导结构回旋行波放大器的结构和工作参数如表1所示,其中 p_v 表示铜的电阻率.

4 结论

本文通过对毫米波回旋行波放大器的绝对不稳定性、回旋返波振荡以及电子注-波互作用的研究,讨论了回旋行波放大器的稳定性、寄生模式的抑制和工作参数的优化等问题,给出了 Ka 波段 TE_{02} 模二次谐波回旋行波放大器的非线性模拟结果:在电子注电压 90kV、电流 25A、横纵速度比 1.2、工作磁场 0.643T 时,分别选取损耗波导段长度 17cm、截止段长度 15cm、铜段长度 6cm. 在速度零散为 3%时,中心频率 35GHz 处可获得 125kW 的输出峰值功率、5.5%的效率和 4.3%的带宽.

REFERENCES

[1] LIU PuKun, XU ShouXi. Review of gyroklystron amplifiers and its development[J]. *J. Electronics and Information technology* (刘濮鲲,徐寿喜. 回旋速调管放大器及其发展评述. 电子信息学报), 2003, **25**(5): 683—694.

[2] LAI Guo-Jun, LIU Pu-Kun. Analysis on velocity of a W-band gyrotron traveling wave amplifier[J]. *J. Infrared Millim. Waves* (来国军,刘濮鲲. W 波段回旋行波管放大器速度零散的分析. 红外与毫米波学报), 2006, **25**(6): 447—450.

[3] Chu K R. Overview of research on the gyrotron traveling-wave amplifier[J]. *IEEE Trans Plasma Sci* 2002, **30**(3): 903—908.

[4] Chu K R, Barnett L R, Chen H Y, *et al* Stabilization of absolute instabilities in the gyrotron traveling wave amplifier [J]. *Phys Rev Lett*, 1995, **74**(7): 1103—1106.

[5] NIU Xin-Jian, GU Ling, YU Sheng, *et al* Corrugated waveguide mode conversion for 94GHz second-harmonic gyrotron[J]. *J. Infrared Millim. Waves* (牛新建,顾玲,喻胜,等. 94GHz 二次谐波回旋管波纹波导模式转换. 红外与毫米波学报), 2007, **26**(2): 117—120.

[6] Wang Q S, McDermott D B, Luhmann N C. Operation of a stable 200 kW second-harmonic gyro-TWT amplifier[J]. *IEEE Trans Plasma Sci*, 1996, **24**(3): 700—706.

[7] Yeh Y S, Hung C L, Su C W, *et al* W-Band second harmonic gyrotron traveling wave amplifer with distributed-loss and severed structures[J]. *Int J. Infrared Millimeter Waves*, 2004, **25**(1): 29—42.

[8] Leon K C. Stable high power TE_{01} Gyro-TWT amplifiers [J]. *IEEE Trans Plasma Sci*, 1994, **22**(5): 585—592.

[9] LAI GuoJun, JIA YunFeng, LIU PuKun. Absolute instability in gyro-traveling-wave tube[J]. *High Power Laser and Particle Beams* (来国军,贾云峰,刘濮鲲. W 波段回旋行波管放大器绝对不稳定性的研究. 强激光与粒子束), 2005, 17(12): 1865—1869.

(上接 6页)

[24] Lin C H, Singer K E, Evans-Freeman J H, *et al* Infrared photoreflectance of InAs[J]. *Semicond. Sci Technol* 1997, **12**, 1619.

[25] Muñoz M, Pollak F H. Temperature dependence of the energy and broadening parameter of the fundamental band gap of GaSb and $Ga_{1-x}In_xAs_ySb_{1-y}$/GaSb ($0.07 < \sim x < \sim 0.22$, $0.05 < \sim y < \sim 0.19$) quaternary alloys using infrared photoreflectance[J]. *Phys Rev* B, 2000, **62**, 16600.

[26] Shao J, Lu W, Yue F, *et al* Photoreflectance spectroscopy with a step-scan Fourier-transform infrared spectrometer: Technique and applications[J]. *Rev Sci Instrum.* 2007, **78**, 013111.

[27] Johnson T J, Zachmann G, *Introduction to Step-Scan FTIR* [M]. Ettlingen: Bruker Optik.

[28] Jiang E Y. *Advanced FT-IR Spectroscopy*[M], Madison: Thermo Electron Corporation, 2003.

[29] Chu J H, Xu S Q, Tang D Y. Energy gap versus alloy composition and temperature in $Hg_{1?x}Cd_xTe$[J]. *Appl Phys Lett* 1983, **43**, 1064.

[30] Shen H, Dutta M. Sweeping photoreflectance spectroscopy of semiconductors[J]. *Appl Phys Lett* 1990, **57**, 587.

[31] Yan D, Qiang H, Pollak F H. A new offset technique for suppression of spurious signals in photoreflectance spectra [J]. *Rev. Sci Instrum.* 1994, **65**, 1988.

[32] Merrick M, Hosea T J C, Murdin B N, *et al* Bandgap bowing in InSb1-xNx investigated with a new Fourier transform modulated spectroscopy technique for the mid-infrared [J]. *AIP Conf Proc* 2005, 772: 295—296.

[33] Berding M A, van Schilfgaarde M A. Sher. First-principles calculation of native defect densities in $Hg_{0.8}Cd_{0.2}Te$ [J]. *Phys Rev B*, 1994, **50**, 1519.